


Article

Effect of Ammonia Addition on the Ignition Delay Mechanism of Methyl Decanoate

Ye Qiu *, Haijun Wei *, Daping Zhou and Jingming Li 

College of Merchant Marine, Shanghai Maritime University, Shanghai 201306, China;
dpzhou@shmtu.edu.cn (D.Z.); jmli@shmtu.edu.cn (J.L.)

* Correspondence: yeqiu@shmtu.edu.cn (Y.Q.); hjwei@shmtu.edu.cn (H.W.); Tel.: +(86)-138-1800-9587 (Y.Q.)

Abstract: In this study, the effect of mixing a small amount of ammonia on the ignition delay time of methyl decanoate under different conditions was studied from the perspective of the combustion mechanism. The effect of adding ammonia on the ignition delay time of methyl decanoate at different pressures and temperatures was studied by means of simulation calculations and numerical comparison. Integrating the detailed mechanism and reaction path of methyl decanoate, the sensitivity of the ignition delay time was investigated. Analyses of the ignition delay time and rate of production were conducted to explore the transformation and influence of ammonia on the oxidation/decomposition process of the main elementary reaction during the ignition of methyl decanoate. The research illustrated that the ignition delay time of methyl decanoate increased with the number of moles of mixed ammonia at a certain temperature range, and in the negative temperature coefficient region, the effect of ammonia on the ignition delay time was the greatest. In addition, the susceptibility and yield analysis of methyl decanoate showed that the addition of ammonia had a weakening effect on the elementary reactions that originally promoted and inhibited methyl decanoate, and its consumption and production rates were reduced.

Keywords: methyl decanoate; ammonia; ignition delay time; sensitivity analysis; rate of production analysis



Citation: Qiu, Y.; Wei, H.; Zhou, D.; Li, J. Effect of Ammonia Addition on the Ignition Delay Mechanism of Methyl Decanoate. *J. Mar. Sci. Eng.* **2022**, *10*, 922. <https://doi.org/10.3390/jmse10070922>

Academic Editor: Spyros Hirdaris

Received: 10 June 2022

Accepted: 1 July 2022

Published: 3 July 2022

Publisher's Note: MDPI stays neutral with regard to jurisdictional claims in published maps and institutional affiliations.



Copyright: © 2022 by the authors. Licensee MDPI, Basel, Switzerland. This article is an open access article distributed under the terms and conditions of the Creative Commons Attribution (CC BY) license (<https://creativecommons.org/licenses/by/4.0/>).

1. Introduction

With the increasingly serious energy crisis and environmental problems, the awareness of environmental protection from all walks of life at home and abroad has been continuously enhanced. As the main source of marine air pollution, ship engine exhaust has attracted more and more attention from governments and regions, and the requirements for controlling the emission of polluting gases have become increasingly strong [1]. In order to protect the marine environment and effectively control the emission of harmful gases, the International Maritime Organization (IMO) and the governments of various countries have issued regulations to limit pollutants and set up emission control areas. Among these, the International Convention for the Prevention of Pollution from Ships issued by the IMO, "Regulations for Prevention of Air Pollution from Ships", clearly stipulated the emission limits of exhaust pollutants from ships' engines and clarified the standards and time limits for the reduction of ship exhaust emissions [2]. "Clean, low-carbon, safe, and efficient" energy reform has become the general trend [3].

In order to reduce environmental pollution and harmful substances emissions, diesel and natural gas dual-fuel engines are the subjects of a development trend in internal combustion engines. However, both diesel and natural gas are nonrenewable energy sources, and excessive exploitation of these leads to resource depletion and vegetation destruction. At the same time, the supply and demand of oil and gas are greatly affected by the international situation, and price fluctuations can intensify, which is not conducive to economic benefits. In addition, diesel–natural gas dual-fuel engines will not meet the

IMO's ambitious goal of reducing carbon dioxide emissions from shipping to 50% of the 2008 levels by 2050.

Biodiesel is a kind of fatty acid ester that can be produced from waste oil. Therefore, it is carbon-neutral, renewable, and easy to degrade. Most importantly, it does not contain sulfur and is nontoxic, so it is an ideal alternative fuel for diesel. It has been proven that the use of biodiesel on ships can effectively reduce the emissions of harmful substances, such as sulfur oxides (SO_x), carbon monoxide (CO), particulate matter (PM), and hydrocarbons (HC) [4]. Methyl decanoate (MD) is an important manifestation of biodiesel [5–7]. Therefore, the research conducted on biodiesel by domestic and international scholars has focused mainly on MD. Herbinet et al. [8] studied the low- and high-temperature oxidation performance of MD, developed the chemical reaction mechanism, and constructed a detailed combustion kinetics model, which was effectively verified in ignition delay and JSR experiments, laying a foundation for the combustion kinetics study of MD. Szybist et al. [9] studied the self-ignition characteristics and heat release laws of MD and other fuels on the engine bench. The study showed that MD produced a large amount of CO_2 during the low-temperature heat release process, which was the result of ester decarboxylation and not oxidation. Wang et al. [10] experimentally measured the oxidation behavior of MD in laminar premixed and nonpremixed flames in a countercurrent structure under atmospheric pressure and compared the experimental data with the experimental data of an n-alkane flame with a similar carbon number to evaluate the influence of saturation, the carbon chain length, and the existence of the ester group on the flame. In addition, Wang Shiye et al. [11] studied the emission performance of a mixed fuel of MD and butanol at high temperature and pressure and concluded that the NO_x emission was reduced. However, under the current background of decarbonization, it is difficult to break through the barrier of carbon reduction simply for the development and research of organic carbon-based fuels.

Ammonia (NH_3), as a zero-carbon fuel, is attracting the attention of scholars. Ammonia combustion is associated with carbon-related air pollutants; black carbon or soot, unburned hydrocarbons (HC), and methane and carbon monoxide (CO) emissions are basically eliminated, and only nitrogen and nitrous compounds are the products of ammonia's complete combustion. Pfahl et al. [12] and Takizawa et al. [13] successively investigated the outward propagation speed of a spherical flame when an ammonia/air mixture was burned at 0.1 MPa. The results showed that the laminar combustion rate of NH_3 was generally lower than that of hydrocarbon fuels. Wang et al. [14] used laser ignition technology to study the laminar combustion characteristics of a premixed ammonia/hydrogen/air mixture and reasonably predicted the accuracy of various mechanism models. Many studies have shown that the poor combustion performance of NH_3 is the main reason for its limited application.

Based on the above, it is believed that MD and NH_3 are highly complementary. Therefore, in this paper, the author propose to mix these two fuels, which could not only improve the quality and performance of their combustion but effectively respond to the energy crisis and climate change. Chemical properties are crucial. At present, there have been relatively few studies on the mixed combustion of these two fuels, and most actual internal combustion engines are in the medium- and low-temperature regions. In this study, referring to the research methods of Liu [15] and Pei [16] and starting from the medium- and low-temperature reaction path of MD, the mixed combustion was studied. The effect of ammonia on the mechanism of the MD ignition delay time (IDT) provides a reference for exploring biodiesel–ammonia dual-fuel engines.

2. Materials and Methods

2.1. Model Selection and Simulation Settings

In this study, the closed homogeneous batch reaction 0-D model (CHBR) in Chemkin was mainly used to calculate the IDT of the methyl caprate/ammonia mixtures.

In order to analyze the effect of ammonia addition on the ignition of methyl decanoate, three fuel components were set, and the total number of fuel moles was specified to be

1 mol. For the first case, the fuel was 1 mol MD, without NH_3 , denoted as 1 mol MD; for the second case, NH_3 was added, denoted as 0.9 mol MD + 0.1 mol NH_3 and 0.8 mol MD + 0.2 mol NH_3 ; and in the third case, N_2 was substituted for NH_3 for comparison, denoted as 1 mol MD + 0.1 mol N_2 and 0.8 mol MD + 0.2 mol N_2 . The equivalent ratio was $\Phi = 1$ in all three cases.

In the simulation study, the initial conditions, such as the composition of the reaction mixture, the initial temperature, and the initial pressure, were as close as possible to the thermodynamic state of a marine diesel engine. At the same time, in order to more accurately judge the ignition time of the fuel, two parameters, those of the reaction temperature rising over 400 K and the first peak of hydroxyl (OH) radicals in the cylinder, were set in Chemkin at the same time. The specific settings of the mixture and parameters are shown in Table 1 below.

Table 1. Conditions, mixture compositions, and parameters: $T = 700\text{--}1100\text{ K}$, $p = 6\text{--}9\text{ MPa}$.

Condition	MD (mol)	NH_3 (mol)	N_2 (mol)	Denoted as
1	1	0	0	1 mol MD
2-1	0.9	0.1	0	0.9 mol MD + 0.1 mol NH_3
2-2	0.8	0.2	0	0.8 mol MD + 0.2 mol NH_3
3-1	0.9	0	0.1	1 mol MD + 0.1 mol N_2
3-2	0.8	0	0.2	0.8 mol MD + 0.2 mol N_2

2.2. Mechanism Selection

The chemical reaction mechanism of methyl decanoate came from the Lawrence Livermore National Laboratory (LLNL), and the detailed mechanism included 2878 species and 8555 reactions. The chemical reaction mechanism of ammonia came from the research results of A. Stagni et al. [17,18] from the CRECK Modeling Group (TCMG). The detailed mechanism included 31 species and 203 reactions. The physical parameters of methyl decanoate and ammonia obtained from the test are compared in Table 2.

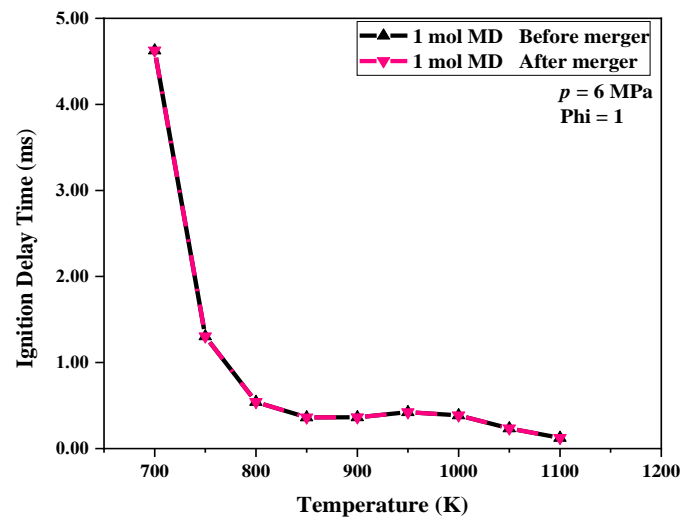
Table 2. Reference table of physical properties of methyl decanoate and NH_3 .

Parameter	MD	NH_3
Formula	$\text{C}_{11}\text{H}_{22}\text{O}_2$	NH_3
Molecular weight	186	17
Octane number	/	110
Lower heating value (MJ/kg)	34	18.8
Density (20 °C)	0.873 (g/cm^3)	0.707 (g/L)
Boiling point (°C)	94	−33.4

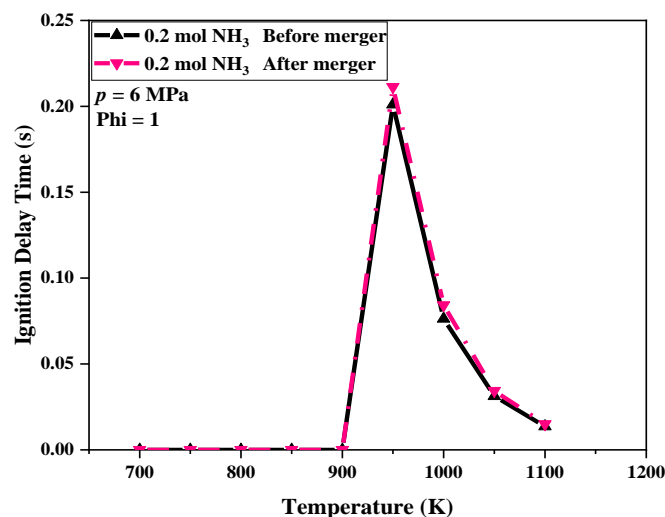
The above mechanisms have been verified by previous researchers to be consistent with the simulation values and experimental performance. After the combination of the two mechanisms, the IDT values were compared under the same conditions as those before the combination, as shown in Figure 1.

Figure 1a shows that IDT data before and after the MD mechanism merger were almost completely coincident under an initial pressure of 6 MPa, equivalent ratio $\Phi = 1$, and initial temperature of 700–1100 K. Figure 1b shows that the IDT values of NH_3 in the initial temperature range of 700–900 K coincided and were all 0, that is, there was no ignition under this initial condition, as determined by the combustion characteristics of NH_3 .

At 950 K and 1100 K, the IDT data before and after the merger did not coincide, but within the margin of error, the deviation was acceptable.



(a)



(b)

Figure 1. (a) Comparison of ignition delay times before and after MD mechanism merger. (b) Comparison of ignition delay times before and after NH₃ mechanism merger.

3. Results and Discussion

3.1. Analysis of Ignition Delay Time

In order to better compare the effect of NH₃ on the IDT of MD, the change curves of the IDT at the initial temperature are shown in Figure 2a–d. It is generally believed that the IDT of a fuel decreases with increasing temperature, but this was not the case for the MD. The IDT of the MD first decreased as the initial temperature increased but then increased and then decreases after 900 K. This was the negative temperature coefficient (NTC) behavior exhibited by MD [19]. It is obvious that the NTC phenomenon of MD appeared between 750 K and 950 K. This was due to the fact that MD with long carbon chains exhibits the properties of alkane groups [20,21].

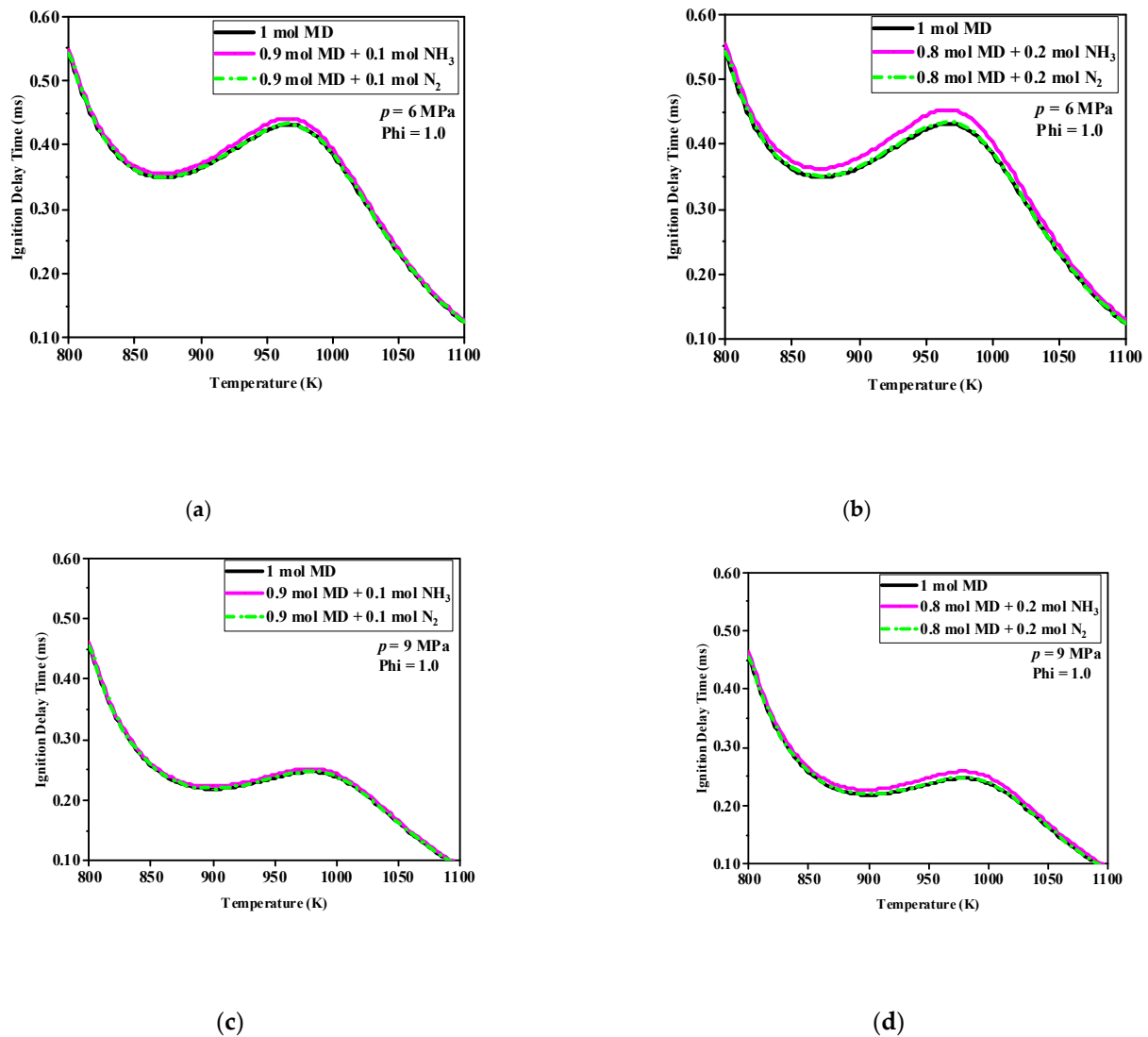


Figure 2. The IDT of each component at an initial temperature of 800–1100 K: (a) 1 mol MD, 0.9 mol MD + 0.1 mol NH_3 , and 0.9 mol MD + 0.1 mol N_2 at $p = 6$ MPa; (b) 1 mol MD, 0.8 mol MD + 0.2 mol NH_3 , and 0.8 mol MD + 0.2 mol N_2 at $p = 6$ MPa; (c) 1 mol MD, 0.9 mol MD + 0.1 mol NH_3 , and 0.9 mol MD + 0.1 mol N_2 at $p = 9$ MPa; (d) 1 mol MD, 0.8 mol MD + 0.2 mol NH_3 , and 0.8 mol MD + 0.2 mol N_2 at $p = 9$ MPa.

Figure 2 shows that under the same conditions, the addition of N_2 had almost no effect on the ignition of MD, that is, the black and green lines of each figure almost overlapped, which also shows that NH_3 was the only material variable that really affected the ignition of MD. As the NH_3 increased, the distance between the purple curve and the other two lines increased, indicating that after MD was mixed with NH_3 , the IDT was prolonged, and it increased as the amount of NH_3 increased, especially in the NTC region, this was because NH_3 absorbed part of the heat and slowed down the oxidation decomposition rate of MD.

Comparing Figure 2a–d shows that when the initial pressure increased from 6 to 9 MPa, the IDT of the MD significantly decreased over the whole temperature range. With the same number of moles of NH_3 , the pressure increased, and the purple curve approached the black and green curves. The reason for this was that the inhibitory effect of the NH_3 on MD ignition was reduced. In addition, the effect of NH_3 addition on the IDT of the MD was mainly concentrated in the temperature region corresponding to the occurrence of the NTC phenomenon in MD.

3.2. Reaction Path and Sensitivity Analysis

3.2.1. The Main Reaction Pathways

The reaction pathway of MD is very similar to that of long-chain hydrocarbons. In Figure 3, the MD low-temperature (L1–L5), medium-temperature (M1–M2), and high-temperature (H) reactions are marked with blue, yellow, and red colors, respectively, and each step represents the same type of reaction. Under low-temperature conditions, the MD was dehydrogenated by the free radicals OH and H to form 10 isomers of methyl decanoate, MDXJ (X = 1, 2, . . . 9, 10), among which the MD and dehydrogenation reaction of the radical OH dominated. The generated MDXJ then oxidized to generate a peroxide group (MDO2), which was then isomerized to form a hydroperoxy group (MDOOH). MDOOH continued to be oxygenated to form a double peroxy hydrogen group (MDOOHO2), and MDOOHO2 decomposed into a free radical OH and ketoester (MDKET). Finally, the ketoester C-C bond was broken and decomposed into small molecular compounds. As the temperature increased, the middle–high temperature reactions were enhanced and competed with the low-temperature reaction, resulting in the backward shift of the MD reaction pathway coupled with the enhancement of the β_1 cleavage reaction. Then, the MD decomposed into the relatively smaller molecules x1 and x2, inhibiting the low-temperature reactivity, interfering with the overall reaction order of the NTC system, and resulting in a prolonged IDT. In the high-temperature region, MD directly sheared β_2 into the relatively smaller molecules y1 and y2, which promoted the depletion and decomposition of MD, and the IDT began to decrease again.

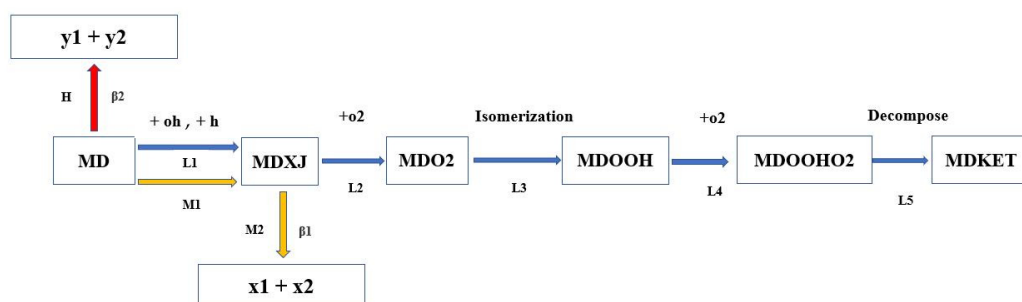


Figure 3. Reaction paths of MD at different temperatures.

3.2.2. Sensitivity Analysis of Ignition Delay Time

Regarding the above discussion, in order to further illustrate the effect of NH₃ on the IDT of MD, a representative reaction was selected, as shown in Table 3, and an IDT mechanism sensitivity analysis was carried out on the mixing of NH₃ into MD.

Table 3. The elementary reactions.

Paths	Number	Elementary Reaction
L1	R1404	md + oh = md7j + h2o
L2	R4117	md7j + o2 = md7o2
L3	R4770	md7o2 = md7ooh5j
L4	R5892	md7ooh5j + o2 = md7ooh5o2
L5	R6257	md7ooh5o2 = mdket75 + oh
M2	R1451	mo7d + c2h5 = md7j
H	R1337	me2j + c8h17-1 = md

Two cases of 1 mol MD and 0.8 mol MD + 0.2 mol NH₃ were selected to study the sensitivity of elementary reactions promoting and inhibiting reactivity at initial temperatures of 800 K, 850 K, 900 K, 950 K, 1000 K, and 1050 K. This range included the low-, medium-, and high-temperature regions and the NTC region. The IDT sensitivity coefficient S_i was

defined per Equation (1), that is, the rate of change in IDT after the reaction constant is doubled:

$$S_i = \frac{\tau(2k_i) - \tau(k_i)}{\tau(k_i)} \quad (1)$$

where τ is the ignition delay period of the mixed fuel, and k_i is the specific rate coefficient of the i th reaction. This means that a positive sensitivity coefficient indicated that the elementary reaction inhibited the ignition of fuel, and a negative value indicated that the reaction promoted ignition. The greater the absolute value of the sensitivity coefficient was, the greater the influence of the reaction on fuel ignition was.

Figure 4a–f is a comparison of the sensitivity changes of the main elements in Table 3 under the conditions of 6 MPa and equivalence ratio $\Phi = 1$. The promotion or inhibition of all reactions in the low–medium temperature range (800–950 K) increased with the temperature, and the R1404 elementary reaction was the most active, indicating that the consumption path of MD in this temperature range was R1404-dominated. However, the activity began to decrease at 950 K. In the NTC behavior region (about 870–970 K), the activity of R1451 increased with the initial temperature, indicating that the inhibitory effect of this reaction on MD ignition was enhanced and reached its maximum at 950 K, which means that starting from 950 K, the consumption of MD with the low-temperature reaction was inhibited, the β_1 cleavage reaction was enhanced, and its reaction channel moved backward to β_1 .

In the medium–high temperature range (950–1050 K), the elementary reactions in the low-temperature reaction were as follows: The activities of R1404, R4117, R4770, R5933, and R6257 decreased as the initial temperature increased and had little effect on the MD at 1050 K. Even at the initial temperature of 1050 K, the sensitivity coefficient of R1404 was positive, which inhibited the reaction activity. In addition, the inhibitory effect of the R1451 reaction with β_1 cleavage on the MD weakened as the initial temperature increased, while the activity of the R1337 reaction with β_2 cleavage was extremely active in this temperature range. This means that in the medium–high temperature range, as the initial temperature increased, the β_1 cleavage reaction of the MD was weakened, the β_2 cleavage reaction was enhanced, and the channel continued to move back to β_2 , which released the inhibitory factor of the MD response, and the IDT was greatly reduced.

As the number of moles of NH_3 increased from 0 to 0.2 mol, the absolute values of the sensitivity coefficients of various elementary reactions at different initial temperatures decreased to varying degrees. Some of the promoting/inhibiting effects were counteracted. Figure 4 also shows that the temperature range where NH_3 weakened the elementary reaction of the MD the most was near the NTC region. This was because, in the NTC region, the MD transformed from a low-temperature chain reaction to a medium- to high-temperature β -cleavage reaction, and the addition of the NH_3 was involved. Therefore, the addition of NH_3 snatched parts of the OH and inhibited the low-temperature chain reaction of MD, resulting in the transfer of a small part of the MD to the β cleavage reaction. At the same time, the medium and high temperatures were not enough to completely crack the MD, which greatly increased the IDT of the MD.

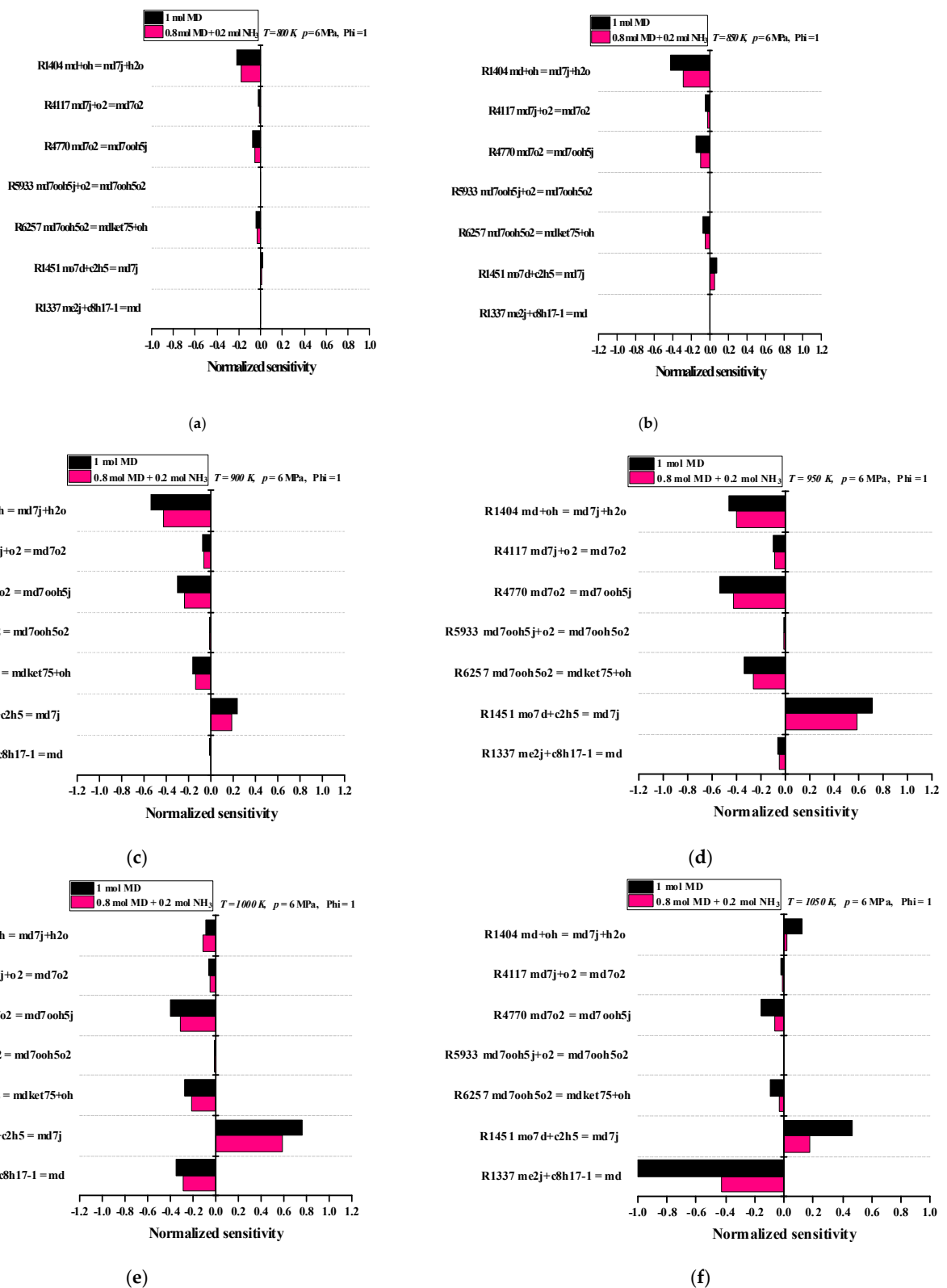


Figure 4. Sensitivity analysis of MD ignition and flame retardation with different moles of NH₃ under the conditions of initial temperature in the range of 800–1050 K and pressure of 1 MPa: (a) initial temperature at 800 K; (b) initial temperature at 850 K; (c) initial temperature at 900 K; (d) initial temperature at 950 K; (e) initial temperature at 1000 K; (f) initial temperature at 1050 K.

3.3. Rate of Production Analysis

The rate of production (ROP) is an important reference for the study of fuel generation and consumption. It constitutes the main basis for the study of fuel reaction paths. Different external conditions have different reaction paths as well as different reaction rates and products. Regarding Figure 3, the key points of low-, medium-, and high-temperature transformation were selected for analysis, and the reaction steps and primitives are shown in Table 4.

Table 4. Key positions of high-temperature transformation in MD and related elementary reaction table.

Paths	Number	Elementary Reaction
L1	R1402	$md + h = md7j + h2$
L1	R1404	$md + oh = md7j + h2o$
L1-L2	R1877	$md7j = md3j$
L2	R4117	$md7j + o2 = md7o2$
L3	R4770	$md7o2 = md7ooh5j$
M2	R1451	$mo7d + c2h5 = md7j$
H	R1337	$me2j + c8h17-1 = md$

Figure 5a–h is an ROP analysis diagram of MD and MD7J under the initial pressures of 6 MPa and 9 MPa and the initial temperatures of 800 K and 950 K. The curve in the figure shows a negative value. This indicates that the corresponding ROP was a consumption reaction; a positive value would indicate production reaction.

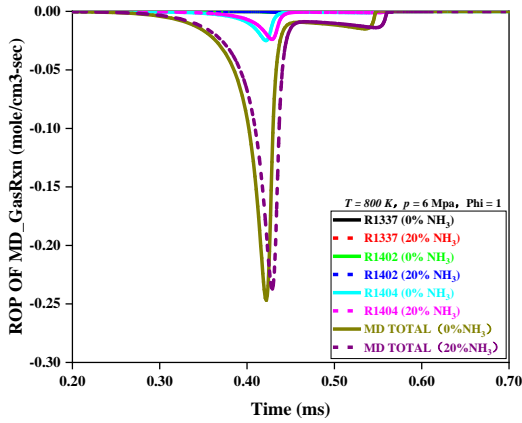
Because of the effect of the initial pressure on the ROP, the MD and MD7J had the same change trend in ROP under different initial pressures. As the initial pressure increased, the absolute value of the ROP was obviously enhanced, indicating that the reaction rate of each primitive accelerated as the initial pressure increased and that the time required for the reaction to reach equilibrium was relatively reduced, that is, the IDT decreased.

Because of the effect of the initial temperature on the ROP, the ROP variation trends of the MD and MD7J were different at different initial temperatures. At the initial low temperature of 800 K, the overall reaction rate trends for the MD and MD7J were consistent with the change trends for the low-temperature reaction channel. The MD was mainly consumed by the dehydrogenation reaction with H and OH to generate the MD7J, and its main elemental reactions were R1402 and R1404, respectively. The dehydrogenation reaction through the OH radical played a dominant role, while the pyrolysis reaction of MD did not exist, that is, the R1337 curve was 0. Correspondingly, the main source of MD7J was R1404, and the MD7J was consumed through oxygenation, pyrolysis, isomerization, and other reactions. The main elemental reactions were R4117, R1451, and R1877, among which the oxidation reaction of R4117 was dominant.

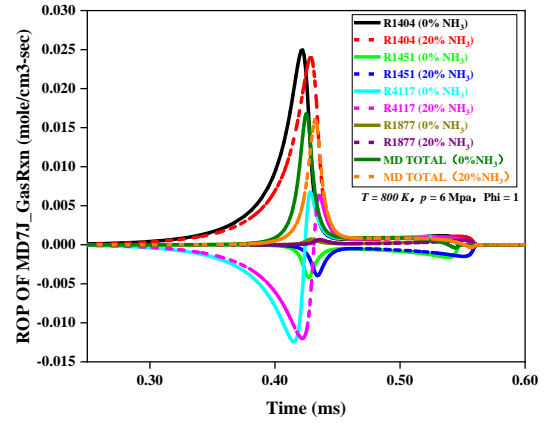
The temperature of 950 K fell inside the range of medium-temperature reaction and was in the NTC region. Compared with those at low temperature, the reactions of MD and MD7J at this initial temperature were relatively complicated. At this initial temperature, the reaction rates of low-temperature primitives, such as R1402, R1404, R1877, R4117, and R4770, dropped sharply or even became zero, and both the MD and MD7J underwent β -cleavage (R1337 and R1451), but the β -cleavage of the MD7J was more significant than that of MD. This indicates that the low-temperature chain reaction and β -cleavage of the MD and MD7J coexisted at 950 K and that there was a competitive relationship.

When the NH_3 mole ratio increased from 0 to 20%, the consumption rate and production rate of MD and its intermediates decreased at the same initial pressure and temperature, and the time required for the reaction to reach equilibrium was relatively prolonged, that is, the IDT increased. At 950 K in the NTC region, it was obvious that the addition of NH_3 had the most sensitive effect on the reaction rate of the MD. The consumption and average production rate of all the elements, including intermediates, decreased the most, and the delay of reaction toward equilibrium reached the maximum, that is, the IDT reached the maximum. This indicates that in the NTC system, the addition of NH_3 had a significant

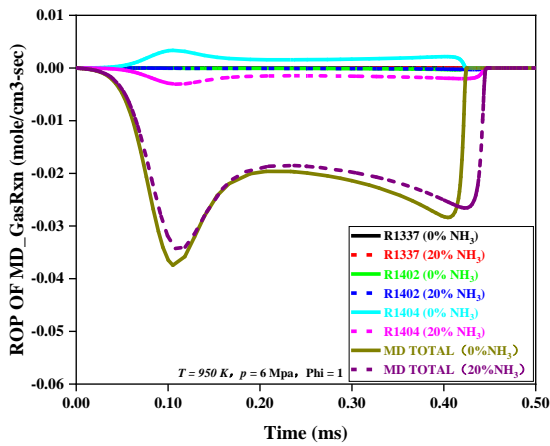
inhibition effect on the MD consumption rate. In practical applications of dual-fuel engine, the fuel injection temperature should be avoided in the NTC region to ensure good maneuverability of a power device.



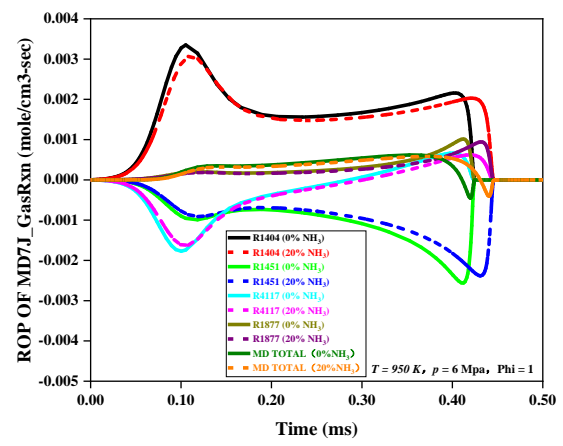
(a)



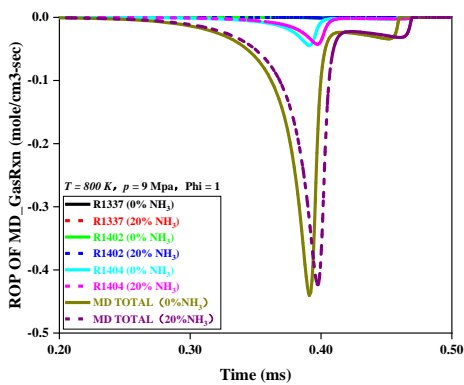
(b)



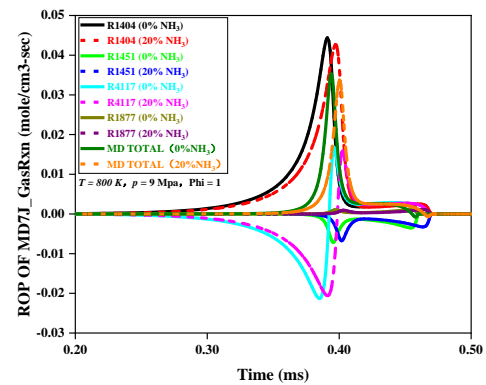
(c)



(d)



(e)



(f)

Figure 5. Cont.

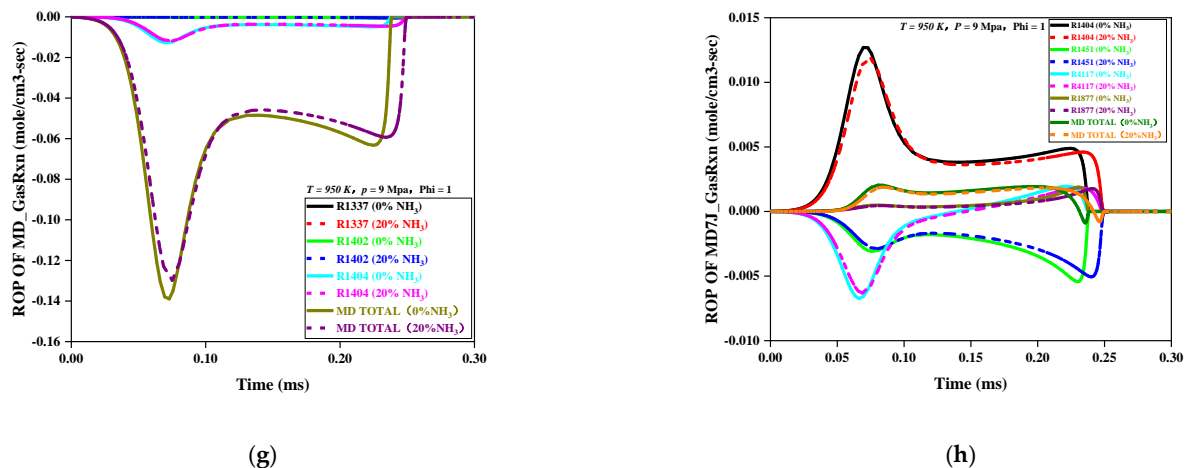


Figure 5. ROP analysis of MD and MD7J with different moles of NH₃ at temperatures of 800 K and 950 K and pressures of 6 MPa and 9 MPa: (a) ROP of MD at T = 800 K and p = 6 MPa; (b) ROP of MD7J at T = 800 K and p = 6 MPa; (c) ROP of MD at T = 950 K and p = 6 MPa; (d) ROP of MD7J at T = 950 K and p = 6 MPa; (e) ROP of MD at T = 800 K and p = 9 MPa; (f) ROP of MD7J at T = 800 K and p = 9 MPa; (g) ROP of MD at T = 950 K and p = 9 MPa; (h) ROP of MD7J at T = 950 K and p = 9 MPa.

4. Conclusions

In this study, the effect of adding NH₃ on the IDT of MD at different pressures and temperatures was studied by means of simulation calculations and numerical comparison. By integrating the detailed mechanism and reaction path of MD, the sensitivity of the IDT was investigated. Analyses of the IDT and ROP were conducted to explore the transformation and influence of NH₃ on the oxidation/decomposition process of the main elementary reaction during the ignition of MD, and the following conclusions could be drawn:

- (1) Under the same pressure and temperature, the IDT of MD increased as the molar fraction of mixed ammonia increased. At the same pressure and different temperatures, the influence of NH₃ on the IDT of MD in the high-temperature zone was weaker than that in the low-temperature zone, and NH₃ had the greatest influence on the IDT of MD in the NTC zone. However, at the same temperature and different pressures, as the environmental pressure increased, the influence of NH₃ addition on the IDT of MD was weakened.
- (2) Sensitivity analysis of the IDT of the elemental reactions showed that the addition of NH₃ weakened the elemental reactions that originally promoted and inhibited MD, especially when the initial temperature was in the NTC region.
- (3) ROP analysis showed that as NH₃ was added, the consumption and production rates of the MD and its key intermediates decreased, the time required for the reaction to reach equilibrium was relatively prolonged, and the IDT increased. Especially in the NTC region, the inhibition of NH₃ on the MD consumption rate reached the maximum. Therefore, in the practical application of a marine dual-fuel engine, the NTC region of fuel should be avoided as far as possible to ensure good maneuverability of the power device and reduce the response delay.

The aforementioned conclusions provide a reference for the development of alternative energy sources and the design of MD–NH₃ dual-fuel engines, as well as a basis for the next step in researching combustion, emission and performance testing on the diesel engine platform.

Author Contributions: Conceptualization, Y.Q. and H.W.; methodology, Y.Q.; software, Y.Q.; validation, Y.Q., H.W. and D.Z.; formal analysis, Y.Q.; investigation, Y.Q.; resources, H.W.; data curation, Y.Q., D.Z. and J.L.; writing—original draft preparation, Y.Q.; writing—review and editing, Y.Q. and

D.Z.; visualization, Y.Q.; supervision, H.W.; project administration, H.W.; funding acquisition, H.W. All authors have read and agreed to the published version of the manuscript.

Funding: This research was funded by the National Natural Science Foundation of China (NSFC), grant number: 51909154, and the Shanghai Commission of Science and Technology (STSC), grant number: 20DZ2252300.

Institutional Review Board Statement: Not applicable.

Informed Consent Statement: Not applicable.

Data Availability Statement: Not applicable.

Acknowledgments: Thanks to NSFC and STSC for their support and funding.

Conflicts of Interest: The funders had no role in the design of the study; in the collection, analyses, or interpretation of data; in the writing of the manuscript, or in the decision to publish the results.

References

1. Thomson, H.; Corbett, J.J.; Winebrake, J.J. Natural Gas as a Marine Fuel. *Energy Policy* **2015**, *87*, 153–167. [[CrossRef](#)]
2. Bai, J.; Zhou, S.; Guo, H. Effect of natural gas intake conditions on dual fuel engine performance. *Mar. Eng.* **2019**, *41*, 162–164+169.
3. Shao, Z.; Yi, B. Current situation and prospect of hydrogen energy and fuel cell development. *Proc. Chin. Acad. Sci.* **2019**, *34*, 469–477.
4. Wu, G.; Jiang, G.; Yan, Z.; Wei, H.; Huang, Z. Experimental study on the emission reduction mechanism of biodiesel used in marine diesel engine. *J. Harbin Eng. Univ.* **2019**, *40*, 468–476.
5. Zhai, Y.; Ao, C.; Feng, B.; Meng, Q.; Zhang, Y.; Mei, B.; Yang, J.; Liu, F.; Zhang, L. Experimental and kinetic modeling investigation on methyl decanoate pyrolysis at low and atmospheric pressures. *Fuel* **2018**, *232*, 333–340. [[CrossRef](#)]
6. Dooley, S.; Curran, H.J.; Simmie, J.M. Autoignition measurements and a validated kinetic model for the biodiesel surrogate, methyl butanoate. *Combust. Flame* **2008**, *153*, 2–32. [[CrossRef](#)]
7. Seshadri, K.; Lu, T.; Herbinet, O.; Humer, S.; Niemann, U.; Pitz, W.J.; Seiser, R.; Law, C.K. Experimental and kinetic modeling study of extinction and ignition of methyl decanoate in laminar non-premixed flows. *Proc. Combust. Inst.* **2009**, *32*, 1067–1074. [[CrossRef](#)]
8. Herbinet, O.; Pitz, W.J.; Westbrook, C.K. Detailed Chemical Kinetic Oxidation Mechanism for a Biodiesel Surrogate. *Combust. Flame* **2008**, *154*, 507–528. [[CrossRef](#)]
9. Szybist, J.P.; Boehman, A.L.; Haworth, D.C.; Koga, H. Premixed ignition behavior of alternative diesel fuel-relevant compounds in a motored engine experiment. *Combust. Flame* **2007**, *149*, 112–128. [[CrossRef](#)]
10. Wang, Y.L.; Feng, Q.; Egolfopoulos, F.N.; Tsotsis, T.T. Studies of C4 and C10 methyl ester flames. *Combust. Flame* **2011**, *158*, 1507–1519. [[CrossRef](#)]
11. Wang, S.-Y.; Yao, L.; Zhang, J.-D. Homogeneous Charge Compression Ignition Combustion and Emissions of Methyl Decanoate and n-Butanol in Low-Speed Diesel Engine. *J. Propuls. Technol.* **2020**, *41*, 2558–2565.
12. Pfahl, U.J.; Ross, M.C.; Shepherd, J.E.; Pasamehmetoglu, K.O.; Unal, C. Flammability limits, ignition energy, and flame speeds in H₂-CH₄-NH₃-N₂O-O₂-N₂ mixtures. *Combust. Flame* **2000**, *123*, 140–158. [[CrossRef](#)]
13. Takizawa, K.; Takahashi, A.; Tokuhashi, K.; Kondo, S.; Sekiya, A. Burning velocity measurements of nitrogen-containing compounds. *J. Hazard. Mater.* **2008**, *155*, 144–152. [[CrossRef](#)]
14. Ning, W.; Shuai, H.; Zhang, Z.; Li, T.; Yi, P.; Wu, D.; Chen, G. Laminar burning characteristics of ammonia/hydrogen/air mixtures with laser ignition. *Int. J. Hydrogen Energy* **2021**, *46*, 31879–31893.
15. Liu, Z.; Zhou, L.; Zhao, W.; Qi, J.; Wei, H. Mechanism of Methane Addition Affects the Ignition Process of n-heptane under Dual Fuel Engine-like Conditions. *J. Therm. Sci.* **2020**, *29*, 1638–1654. [[CrossRef](#)]
16. Pei, Y.; Zheng, C.; Zhang, B. Chemical kinetic model construction and path analysis of biodiesel substitute mixture. *J. Physicochem.* **2014**, *30*, 217–226.
17. Stagni, A.; Cavallotti, C.; Arunthanayothin, S.; Song, Y.; Herbinet, O.; Battin-Leclerc, F.; Faravelli, T. An experimental theoretical and kinetic-modeling study of the gas-phase oxidation of ammonia. *React. Chem. Eng.* **2020**, *5*, 696–711. [[CrossRef](#)]
18. Song, Y.; Marrodán, L.; Vin, N.; Herbinet, O.; Assaf, E.; Fittschen, C.; Stagni, A.; Faravelli, T.; Alzueta, M.U.; Battin-Leclerc, F. The sensitizing effects of NO₂ and NO on methane low temperature oxidation in a jet stirred reactor. *Proc. COMB* **2019**, *37*, 667–675. [[CrossRef](#)]
19. Hoffman, S.R.; Abraham, J. A comparative study of n-heptane, methyl decanoate, and dimethyl ether combustion characteristics under homogeneous-charge compression-ignition engine conditions. *Fuel* **2009**, *88*, 1099–1108. [[CrossRef](#)]
20. Wang, W.; Yu, L.; Feng, Y.; Qian, Y.; Ju, D.; Lu, X. Autoignition study of methyl decanoate using a rapid compression machine. *Fuel* **2020**, *266*, 117060. [[CrossRef](#)]
21. Li, Z.; Lu, X.; Huang, Z. Autoignition of methyl decanoate/alcohol and ethanol. *J. Shanghai Jiaotong Univ.* **2013**, *47*, 1790–1794.